Journal of Organometallic Chemistry 880 (2019) 341–348

Contents lists available at ScienceDirect

Journal of Organometallic Chemistry

journal homepage: www.elsevier.com/locate/jorganchem

The Sn–C bond reactivity in 1,1-bis(heteroaryl)-2-triorganostannylethanes toward tungsten carbonyl derivatives

Geng-Wen Yin, Huan Yang, Wei-Yi Guo, Liang-Fu Tang*

State Key Laboratory of Elemento-Organic Chemistry, College of Chemistry, Nankai University, Tianjin, 300071, People's Republic of China

ARTICLE INFO

Article history:
Received 11 October 2018
Received in revised form
18 November 2018
Accepted 24 November 2018
Available online 26 November 2018

Keywords:
N ligand
Organotin
Tungsten carbonyl
Oxidative addition
Transition metal–tin complex

ABSTRACT

Reaction of $R_3SnCH_2CH(3,5\text{-}Me_2Pz)_2$ (R = *n*-Bu, CH_2Ph or Ph; Pz = pyrazol-1-yl) with $W(CO)_5THF$ in refluxing THF resulted in the oxidative addition of the inactive R_3Sn–C bond to the tungsten atom to yield metal-metal bonded complexes $CH_2CH(3,5\text{-}Me_2Pz)_2W(CO)_3SnR_3$. While reaction of $R_3SnCH_2CH(mim)_2$ (R = *n*-Bu or Ph; mim = 1-methylimidazol-2-yl) with $W(CO)_6$ in refluxing dioxane gave only the decarbonylation complexes $R_3SnCH_2CH(mim)_2W(CO)_4$, no analogous oxidative addition of the R_3Sn–C bond was observed. In addition, the reactivity of $R_3SnCH_2CH(py)_2$ (R = *n*-Bu or Ph; py = 2-pyridinyl) toward $W(CO)_5THF$ markedly depended on the substituent R. The decarbonylation complex $(n\text{-}Bu)_3SnCH_2CH(py)_2W(CO)_4$ was obtained when R represented the *n*-butyl group, and the oxidative addition reaction of the inactive Ph_3Sn–C bond took place to give $CH_2CH(py)_2W(CO)_3SnPh_3$ when R was the phenyl group. It is interesting that treatment of $(n\text{-}Bu)_3SnCH_2CH(py)_2W(CO)_4$ with I_2 led to the unusual reactivity of the $(n\text{-}Bu)_3Sn$–C bond to afford complex $CH_2CH(py)_2W(CO)_3I$ with the loss of the organotin group. All these newly synthesized compounds were characterized by IR, NMR and elemental analysis, and their structures were unambiguously confirmed by X-ray crystallography.

1. Introduction

The metal mediated Sn–C bond activation, cleavage and transformations have been widely used in diverse synthetic organic chemistry, such as the Stille cross-coupling reaction [1–3] and the carbostannylation of alkynes [4,5]. The reactivity of Sn–C bond toward a transition metal center is essential for these chemical processes, and oxidative addition reactions are important steps in these transformations [3,6,7]. In addition, the oxidative addition of the Sn–C bond toward low valent transition metal compounds is a useful method to generate various transition metal-tin complexes [8–14], which have been extensively used as highly efficient heterobimetallic catalysts in various organic reactions [15,16]. In many cases, the reactivity of Sn–C bond is related to the electronegativities of substituents on the tin atom [3]. For example, the cleavage of the $Sn–C_{aryl}$ bond is faster than that of $Sn–C_{alkyl}$ bond [3,8]. Our previous work showed that the reaction of triarylstannylbis(3,5-dimethylpyrazol-1-yl)methanes with $W(CO)_5THF$ resulted in the oxidative addition of the $Sn–C_{sp3}$ bond to the tungsten(0) atom, while the similar reaction of trialkylstannylbis(3,5-dimethylpyrazol-1-yl)methanes did not occur [17,18], suggesting that the electronic effects of the aryl groups on the tin atom play a key role in the oxidative addition reaction. As part of our ongoing interest in functionalized bis(pyrazol-1-yl)alkane ligands, we herein report the synthesis of 1,1-bis(3,5-dimetylpyrazol-1-yl)-2-triorganostannylethanes $[R_3SnCH_2CH(3,5\text{-}Me_2Pz)_2]$, 1,1-bis(1-methylimidazol-2-yl)-2-triorganostannylethanes $[R_3SnCH_2CH(mim)_2]$ and 1,1-bis(pyridyl-2-yl)-2-triorganostannylethanes $[R_3SnCH_2CH(py)_2]$ along with their reactions with tungsten carbonyl derivatives. The R_3Sn–C bond reactivity in $R_3SnCH_2CH(3,5\text{-}Me_2Pz)_2$ is markedly different from that of $R_3SnCH(3,5\text{-}Me_2Pz)_2$ with the short linkage between the tin atom and the donor atoms.

2. Results and discussion

2.1. Synthesis and reaction of $R_3SnCH_2CH(3,5\text{-}Me_2Pz)_2$

$R_3SnCH_2CH(3,5\text{-}Me_2Pz)_2$ were easily obtained in excellent yields by the hydrostannylation of $CH_2{=}C(3,5\text{-}Me_2Pz)_2$ (Pz = pyrazol-1-yl) with R_3SnH (R = *n*-Bu, $PhCH_2$ or Ph) (Scheme 1). Reactions of these three ligands with $W(CO)_5THF$ in refluxing THF resulted in the oxidative addition of the inactive $R_3Sn–C_{sp3}$ bond to the tungsten(0) center to give five-membered metallacyclic complexes **1**–**3**.

* Corresponding author.
E-mail address: lftang@nankai.edu.cn (L.-F. Tang).

https://doi.org/10.1016/j.jorganchem.2018.11.029
0022-328X/

The reactions of $\mathbf{L^1}$ and $\mathbf{L^2}$ are in contrast to the similar reaction of trialkylstannylbis(3,5-dimethylpyrazol-1-yl)methanes [$R_3SnCH(3,5\text{-}Me_2Pz)_2$] [17], in which no analogous oxidative addition of the $R_3Sn{-}C_{sp3}$ bond is observed, although the $R_3Sn{-}C_{sp3}$ bond in $R_3SnCH(3,5\text{-}Me_2Pz)_2$ is relatively active owing to it locating in the α-position of the heteroaryl group. The small ring strain in **1** and **2** as well as the chelate assisted effect of ligands may be the driving force of the reaction of the inactive $R_3Sn{-}C_{sp3}$ bond in $\mathbf{L^1}$ and $\mathbf{L^2}$ in comparison with that in $R_3SnCH(3,5\text{-}Me_2Pz)_2$.

Complexes **1**–**3** have been characterized by elemental analysis, IR and NMR spectroscopies. Three typical metal carbonyl stretching bands in the range 1821–1958 cm^{-1} were observed in their IR spectra, which is similar to those reported in the tricarbonyltungsten species [17]. The methylene proton signals of the WCH_2CH group in **1**–**3** are significantly shifted to higher field compared with the corresponding signals in the free ligands $\mathbf{L^1}$–$\mathbf{L^3}$, such as 0.58 ppm in **2** and 1.63 ppm in $\mathbf{L^2}$. Another obvious change is that the ^{119}Sn NMR signals in **1**–**3** are considerably shifted to lower field compared with those in $\mathbf{L^1}$–$\mathbf{L^3}$, such as 86.5 ppm in **1** and −22.2 ppm in $\mathbf{L^1}$. These changes are consistent with the R_3Sn group transferring from the methylene group to the tungsten atom.

The structures of **2** and **3** have also been confirmed by X-ray crystallography, and are presented in Figs. 1 and 2, which show that the triorganostannyl groups in $\mathbf{L^2}$ and $\mathbf{L^3}$ have been transferred to the tungsten center in **2** and **3**. These two complexes share a similar fundamental framework. For example, 2,2-bis(3,5-dimethylpyrazol-1-yl)ethide acts as a tridentate, monoanionic κ^3-[N,C,N] chelating ligand to result in the formation of two five-membered metallaheterocycles. The X-ray data reveal that complexes **2** and **3** possess analogous structural parameters, such as similar W–Sn, W–N and $W{-}C_{sp3}$ bond distances, as well as N–W–N and C–C–W angles. The W–Sn (2.8235(8) Å in **2** and 2.7887(8) Å in **3**) bond distances are slightly longer than those reported in four-membered metallaheterocyclic complexes $CH(3,4,5\text{-}Me_3Pz)_2W(CO)_3SnPh_3$ (2.7795(4) Å) [11] and $CH(3,5\text{-}{}^iPr_2Pz)_2W(CO)_3SnPh_3$ (2.7712(8) Å) [17], but within the normal range for W–Sn bonds [16]. The $W{-}C_{sp3}$ bond distances are 2.293(5) Å in **2** and 2.306(3) Å in **3**, slightly shorter than the values in $CH(3,4,5\text{-}Me_3Pz)_2W(CO)_3SnPh_3$ (2.326(5) Å) [11] and $CH(3,5\text{-}{}^iPr_2Pz)_2W(CO)_3SnPh_3$ (2.343(6) Å) [17]. In addition, an unsymmetrically semibridging carbonyl between the W–Sn bond is observed in both complexes. The Sn(1)···C(3) distance is 2.719(7) Å for **2** and 2.708(3) Å for **3**, respectively, considerably shorter than the sum of the van der Waals radii for the Sn and C atoms [19], indicating the Sn···C interactions in **2** and **3**. Moreover, this intramolecular Sn···C interactions possibly lead to significant deviations from the tetrahedral geometry for the tin atom and the linearity for the W–C–O angle in both complexes, evidenced by the C(16)–Sn(1)–C(23) angle of 104.3 (3)° in **2** and the C(16)–Sn(1)–C(22) angle of 103.0(1)° in **3** as well as the W(1)–C(3)–O(3) angle of 173.4(6)° in **2** and 173.7(2)° in **3**.

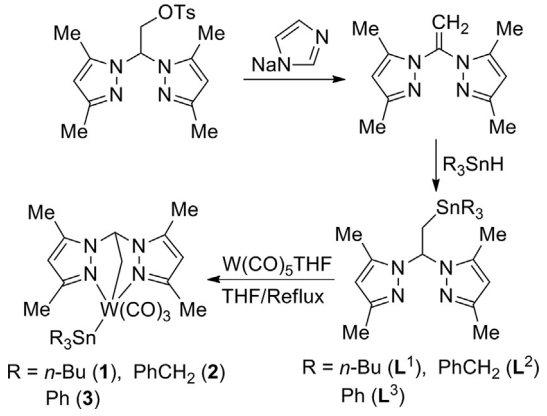

Scheme 1. Synthesis and reaction of $R_3SnCH_2CH(3,5\text{-}Me_2Pz)_2$.

2.2. Reaction of $R_3SnCH_2CH(mim)_2$ and $R_3SnCH_2CH(py)_2$

$R_3SnCH_2CH(mim)_2$ ($\mathbf{L^4}$ and $\mathbf{L^5}$) and $R_3SnCH_2CH(py)_2$ ($\mathbf{L^6}$ and $\mathbf{L^7}$) were obtained similarly by the hydrostannylation of $CH_2{=}C(mim)_2$ (mim = 1-methylimidazol-2-yl) and $CH_2{=}C(py)_2$ (py = 2-pyridinyl) with R_3SnH (R = *n*-Bu or Ph) as described above for $\mathbf{L^1}$–$\mathbf{L^3}$. The reactivity of $\mathbf{L^4}$ and $\mathbf{L^5}$ with tungsten carbonyl derivatives is significantly different from that of $\mathbf{L^1}$–$\mathbf{L^3}$ (Scheme 2). The reactions of $\mathbf{L^4}$ and $\mathbf{L^5}$ with $W(CO)_5THF$ hardly took place, and heating $\mathbf{L^4}$ and $\mathbf{L^5}$ with $W(CO)_6$ even at higher temperature only yielded the decarbonylation complexes **4** and **5**. No oxidative addition products were obtained in these reactions. Complexes **4** and **5** have been characterized by IR and NMR spectra, and for **4** X-ray diffraction analyses.

The IR spectra of **4** and **5** are different from those of **1**–**3**. Four bands in the carbonyl stretching region (1801–1997 cm^{-1}) are observed in **4** and **5**, and these values of ν(CO) can be compared with those reported previously for $CH_2(min)_2M(CO)_4$ (M = Mo or W) [20], indicating a typical *cis*-tetracarbonyl arrangement [21]. The methylene proton signals of the R_3SnCH_2CH group and the ^{119}Sn NMR signals in **4** and **5** are only slightly upfield shifted when compared to the corresponding signals in the free ligands $\mathbf{L^4}$ and $\mathbf{L^5}$, consistent with the R_3SnCH_2CH group away from the reaction center in this reaction. The structure of **4** is shown in Fig. 3, which clearly shows that ligand $\mathbf{L^4}$ acts as a chelating bidentate ligand to the tungsten atom, resulting in a boat conformation of six-membered metallacycle, similar to that in $CH_2(min)_2W(CO)_4$ [20]. The W–N distances are 2.250(6) and 2.260(6) Å, comparable to those in $CH_2(min)_2W(CO)_4$ (2.258(4) and 2.261(5) Å) [20]. Two *cis*-carbonyls C(1)O(1) and C(3)O(3) are distorted with the angles W(1)–C(1)–O(1) of 171.1(7)° and W(1)–C(3)–O(3) of 170.2(8)°. The angles C(10)–C(9)–C(14) of 115.8(6)° and C(9)–C(14)–Sn(1) of 123.3(6)° indicate that the C(9) and C(14) atoms significantly deviate from the tetrahedral geometry. These data disclose the presence of large steric repulsion in this complex.

The reaction of $\mathbf{L^6}$ and $\mathbf{L^7}$ with $W(CO)_5THF$ highly depends on the substituents attached to the tin atom. Like $\mathbf{L^4}$ and $\mathbf{L^5}$, $\mathbf{L^6}$ gave

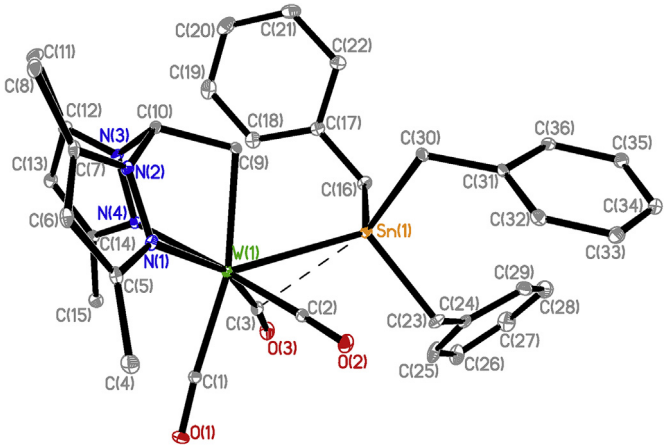

Fig. 1. The molecular structure of **2**. The thermal ellipsoids are drawn at the 30% probability level. Selected bond distances (Å) and angles (°): W(1)–Sn(1) 2.8235(8), W(1)–C(9) 2.293(5), W(1)–N(1) 2.229(5), W(1)–N(4) 2.251(4), Sn(1)···C(3) 2.719 (7) Å; N(1)–W(1)–N(4) 78.4(2), C(10)–C(9)–W(1) 101.6(4), N(2)–C(10)–N(3) 108.1(5), C(16)–Sn(1)–W(1) 113.9(2), C(16)–Sn(1)–C(23) 104.3(3), W(1)–C(3)–O(3) 173.4(6)°.

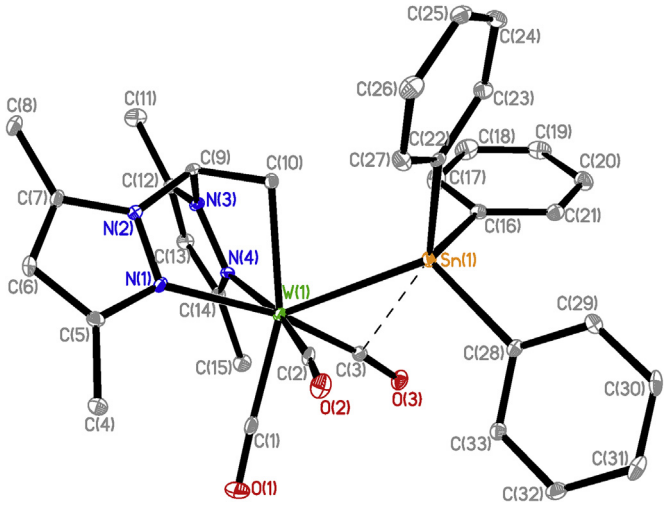

Fig. 2. The molecular structure of **3**. The thermal ellipsoids are drawn at the 30% probability level. Selected bond distances (Å) and angles (°): W(1)–Sn(1) 2.7887(8), W(1)–C(10) 2.306(3), W(1)–N(1) 2.212(2), W(1)–N(4) 2.234(2), Sn(1)···C(3) 2.708 (3) Å; N(1)–W(1)–N(4) 79.57(8), C(9)–C(10)–W(1) 100.7(2), N(2)–C(9)–N(3) 107.8(2), C(22)–Sn(1)–W(1) 115.40(7), C(16)–Sn(1)–C(22) 103.0(1), W(1)–C(3)–O(3) 173.7(2)°.

only the decarbonylation complex **6** upon the alkyl substituents on the tin atom (Scheme 2). However, the similar reaction of $\mathbf{L^7}$ with the phenyl substituents on the tin atom resulted in the oxidative addition of the $Ph_3Sn–C_{sp3}$ bond to the tungsten(0) center to give complex **7**, similar to the reaction of $\mathbf{L^1}$–$\mathbf{L^3}$. Moreover, direct irradiation of $\mathbf{L^7}$ with $W(CO)_6$ at room temperature also yielded the oxidative addition product **7** along with the decarbonylation complex **8**. Obviously, the relatively strong electron-withdrawing ability of the aryl groups in $\mathbf{L^7}$ than the alkyl groups in $\mathbf{L^6}$ plays a key role for the oxidative addition of the $Ph_3Sn–C_{sp3}$ bond in $\mathbf{L^7}$.

The IR and NMR spectra of **6**–**8** are in agreement with the suggested structures. For example, four characteristic infrared absorptions of carbonyl stretching vibrations were observed in **6** and **8**, analogous to **4** and **5**. While only three strong carbonyl stretching absorptions were found in **7**, similar to **1**–**3**. No considerable chemical shift changes were observed when comparing the proton and ^{119}Sn NMR spectra of **6** and **8** with the free ligands $\mathbf{L^6}$ and $\mathbf{L^7}$, respectively. The methylene proton signal in **7** (1.70 ppm) is significantly shifted to upfield, compared with that in $\mathbf{L^7}$ (2.25 ppm). The obvious change of the ^{119}Sn chemical shift also was observed between **7** (22.8 ppm) and $\mathbf{L^7}$ (−120.9 ppm), and the value in **7** is very similar to that in **3** (22.1 ppm).

The structures of **6** and **7** have been further confirmed by X-ray structural analyses, and are presented in Figs. 4 and 5, respectively. Fig. 4 shows that the fundamental fragment of **6** is very similar to that in **4**, and these two complexes also share some analogous structural parameters, such as similar W–N bond distance and N–W–N angle. The W–N bond distances in **6** (2.279(7) Å and 2.283(6) Å) are comparable to those of other known pyridyl nitrogen-ligated tungsten(0) complexes [22]. The nonlinear angles W(1)–C(3)–O(3) of 168.7(8)° and W(1)–C(4)–O(4) of 172.3(7)° and the twisted angles of C(15)–C(16)–Sn(1) of 117.5(6)° and C(14)–C(15)–C(16) of 115.9(7)° demonstrate the presence of steric repulsion in **6**, as that in **4**. On the other hand, Fig. 5 clarifies that the structure of **7** is analogous to complexes **2** and **3**. Like 2,2-bis(3,5-dimethylpyrazol-1-yl)ethide in **2** and **3**, 2,2-bis(pyridyl-2-yl) ethide acts as a tridentate, monoanionic κ^3-[N,C,N] chelating ligand in **7**. The W–Sn bond distance (2.792(1) Å) in **7** is very close to that of **3**. A notable difference between **7** and **2** as well as **3** is no unsymmetrically semibridging carbonyl across the W–Sn bond in **7**. The Sn(1)···C(1) distance is 2.798(9) Å in **7**, longer than the corresponding values in **2** and **3**, but still shorter than the sum of the van der Waals radii for the Sn and C atoms [19], indicating that weak Sn···C interaction still exists in **7**, which possibly leads to the deviations from the tetrahedral geometry for the tin atom and the linearity for the W(1)–C(1)–O(1) angle, as observed in **2** and **3**.

2.3. Reaction of **6** and **7** with I_2

Complexes **6** and **7** show interesting structural features. For example, they have two reactive centers toward electrophilic reagents, namely the Sn–C bond and the tungsten(0) center in **6** as

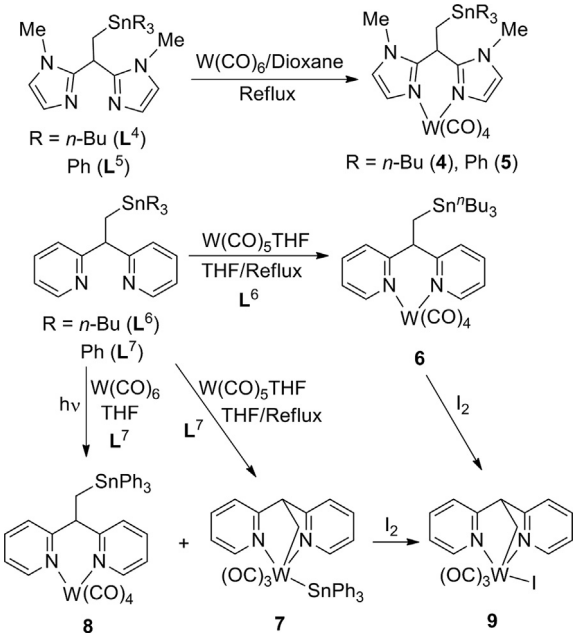

Scheme 2. Reaction of $R_3SnCH_2CH(mim)_2$ and $R_3SnCH_2CH(py)_2$.

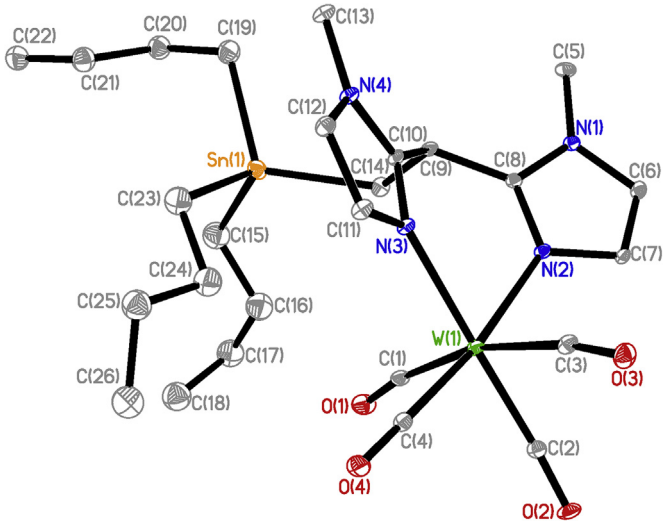

Fig. 3. The molecular structure of **4**. The thermal ellipsoids are drawn at the 30% probability level. Selected bond distances (Å) and angles (°): W(1)–N(2) 2.260(6), W(1)–N(3) 2.250(6), C(9)–C(14) 1.513 (10) Sn(1)–C(14) 2.180(8) Å; N(2)–W(1)–N(3) 78.6(2), C(9)–C(14)–Sn(1) 123.3(6), C(10)–C(9)–C(14) 115.8(6), C(14)–Sn(1)–C(19) 113.1(8), W(1)–C(1)–O(1) 171.1(7), W(1)–C(2)–O(2) 176.3(7), W(1)–C(3)–O(3) 170.2(8), W(1)–C(4)–O(4) 177.4(8)°.

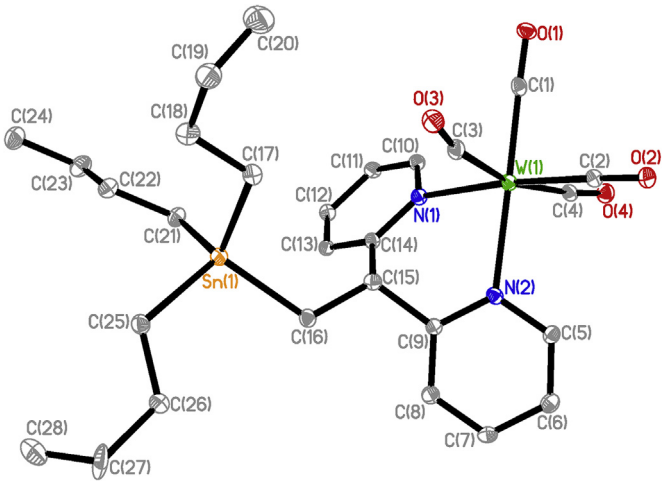

Fig. 4. The molecular structure of **6**. The thermal ellipsoids are drawn at the 30% probability level. Selected bond distances (Å) and angles (°): W(1)–N(1) 2.283(6), W(1)–N(2) 2.279(7), C(15)–C(16) 1.513 (11), Sn(1)–C(16) 2.162(8) Å; N(1)–W(1)–N(2) 79.9(2), C(14)–C(15)–C(16) 115.9(7), C(15)–C(16)–Sn(1) 117.5(6), C(16)–Sn(1)–C(21) 113.8(3), W(1)–C(1)–O(1) 178.1(7), W(1)–C(2)–O(2) 177.6(8), W(1)–C(3)–O(3) 168.7(8), W(1)–C(4)–O(4) 172.3(7)°.

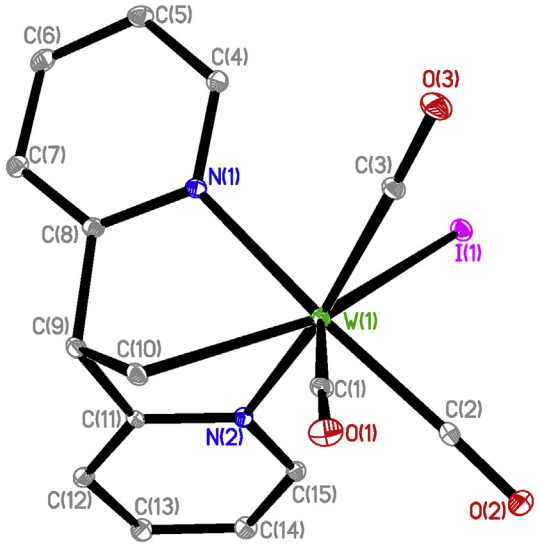

Fig. 6. The molecular structure of **9**. The thermal ellipsoids are drawn at the 30% probability level. Selected bond distances (Å) and angles (°): W(1)–N(1) 2.249(5), W(1)–N(2) 2.273(5), W(1)–C(10) 2.281(6), W(1)–I(1) 2.876(1) Å; N(1)–W(1)–N(2) 82.7(2), C(9)–C(10)–W(1) 100.6(4), C(10)–C(9)–C(11) 105.1(6), W(1)–C(1)–O(1) 178.0(6), W(1)–C(2)–O(2) 177.4(5), W(1)–C(3)–O(3) 178.3(8)°.

well as the Sn–W and W–C_{sp3} bonds in **7**. The cleavage of the Sn–C bond [23] or tin–transition metal bond [16,18] with halogen has been used to synthesize various organic halides. The oxidation of low-valent group 6 metal carbonyl complexes with poly(pyrazol-1-yl)methanes by halogen has been reported in the literature [24–26]. These results inspire us to explore the reactions of complexes **6** and **7**. It is interesting that treatment of **6** with I_2 leads to the unusual reactivity of the (n-Bu)$_3$Sn–C bond to give 2,2-bis(pyridyl-2-yl)ethide tungsten complex (**9**) with the loss of the organotin group from the methylene carbon, which is also obtained by the reaction of **7** with I_2 (Scheme 2). The structure of **9** is confirmed by X-ray single-crystal diffraction, and shown in Fig. 6, which clearly shows that the methylene carbon is bond to the tungsten atom, resulting in 2,2-bis(pyridyl-2-yl)ethide acting as a tridentate κ^3-[N,C,N] chelating ligand, as in **7**. The average W–N distance is 2.261 Å, similar to that in **7** (2.258(7) Å). The W–C_{sp3} bond distance is 2.281(6) Å, slightly shorter than the corresponding bond in **7** (2.293(12) Å).

The possible formation pathways of **9** from **6** are suggested in Scheme 3. According to the known facts, the initial reaction possibly occurs on the tin atom to yield intermediate **A** [23], which subsequently undergoes intramolecular oxidative addition of the C–I bond to the tungsten(0) atom to generate **6** [27–29]. In the alternative possible pathway, the initial reaction possibly happens on the tungsten(0) atom to give intermediate **B** [26], in which the lone electron pair on one iodine atom subsequently attacks the tin atom to facilitate the cleavage of the Sn–C bond, and the resulting intermediate attacks the tungsten atom to impel the cleavage of this W–I bond to give **6**, along with (n-Bu)$_3$SnI leaving.

In conclusion, the Sn–C bond reactivity in 1,1-bis(heteroaryl)-2-triorganostannylethanes toward tungsten carbonyl derivatives has

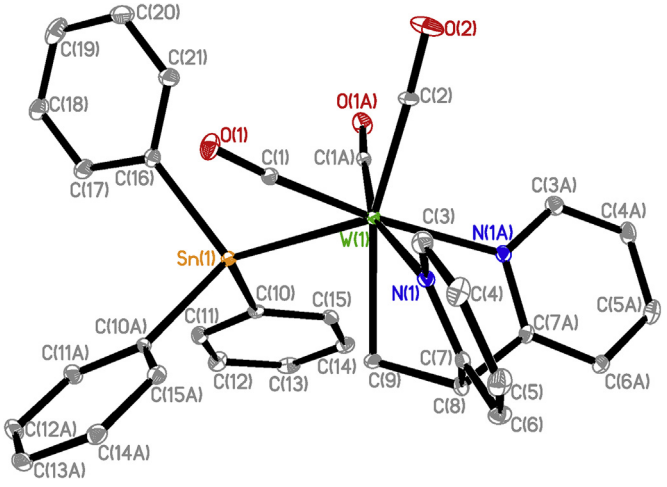

Fig. 5. The molecular structure of **7**. The thermal ellipsoids are drawn at the 30% probability level. Selected bond distances (Å) and angles (°): W(1)–Sn(1) 2.792(1), W(1)–C(9) 2.293(12), W(1)–N(1) 2.258(7), Sn(1)···C(1) 2.798 (9) Å; N(1)–W(1)–N(1A) 79.4(4), C(8)–C(9)–W(1) 99.3(8), C(7)–C(8)–C(7A) 107.7(10), C(16)–Sn(1)–W(1) 115.2(4), W(1)–C(1)–O(1) 175.4(8), W(1)–C(2)–O(2) 177.6(14)°. Symmetric code: A = x, $-y + 1/2$, z.

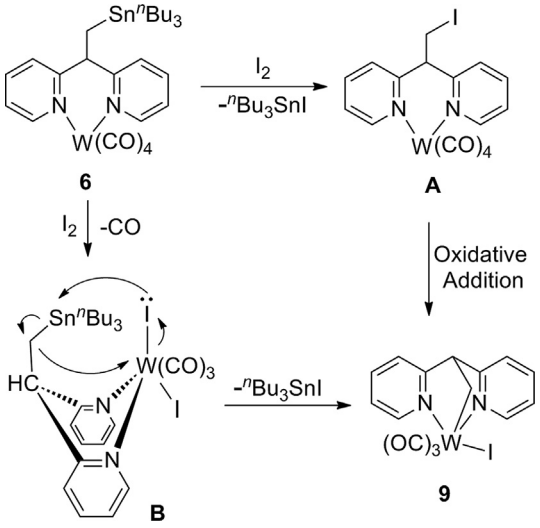

Scheme 3. The possible formation pathways of **9** from **6**.

been investigated, indicating that these ligands with the elongated linkage between the tin atoms and the donor atoms display versatile reactivities. Furthermore, it seems that the lengthened carbon chain in $R_3SnCH_2CH(3,5\text{-}Me_2Pz)_2$ is in favor of the oxidative addition of the inactive $R_3Sn{-}C_{sp3}$ bond, compared to that in $R_3SnCH(3,5\text{-}Me_2Pz)_2$. The $(n\text{-}Bu)_3Sn{-}C$ bond in the decarbonylation complex $(n\text{-}Bu)_3SnCH_2CH(py)_2W(CO)_4$ also shows interesting reactivity toward electrophilic reagent possibly owing to the cooperation effect of two reactive centers.

3. Experimental

All reactions were carried out under an atmosphere of argon. Solvents were dried by standard methods and freshly distilled prior to use. NMR spectra were recorded on a Bruker 400 spectrometer using $CDCl_3$ as the solvent unless otherwise stated, and the chemical shifts were reported in ppm with respect to the reference (internal $SiMe_4$ for ^1H and ^{13}C NMR spectra, external $SnMe_4$ for ^{119}Sn NMR). IR spectra were recorded as KBr pellets on a Tensor 27 spectrometer. Elemental analyses were carried out on an Elementar Vario EL analyzer. $HOCH_2CH(3,5\text{-}Me_2Pz)_2$ [30], $CH_2{=}C(mim)_2$ [20] and $CH_2{=}C(py)_2$ [31] were prepared according to the literature method.

3.1. Synthesis of $TsOCH_2CH(3,5\text{-}Me_2Pz)_2$

Tosyl chloride (1.22 g, 6.4 mmol) was added to the stirred solution of $HOCH_2CH(3,5\text{-}Me_2Pz)_2$ (1.01 g, 4.3 mmol) in pyridine (10 ml). After stirring for 12 h at room temperature, water (30 ml) was added to generate a white precipitate, and the pH value of the mixture was adjusted to 4 with dilute hydrochloric acid. The resulting white precipitate was filtered off, washed with water and dried in vacuo to give $TsOCH_2CH(3,5\text{-}Me_2Pz)_2$ as white powder. Yield: 1.1 g (66%). ^1H NMR: δ 7.66 (d, $J = 8.0$ Hz, 2H, C_6H_4), 7.29 (d, $J = 8.0$ Hz, 2H, C_6H_4), 6.38 (t, $J = 6.6$ Hz, 1H, C*H*), 5.77 (s, 2H, H^4 of pyrazole), 4.97 (d, $J = 6.6$ Hz, 2H, CH_2), 2.43 (s, 3H, CH_3), 2.20 (s, 6H, CH_3), 2.14 (s, 6H, CH_3) ppm. ^{13}C NMR: δ 148.8, 145.0, 139.7, 132.3, 129.9, 128.0 (C^3 and C^5 of pyrazole as well as C_6H_4), 106.8 (C^4 of pyrazole), 68.8, 67.6 (*C*H and CH_2), 21.7, 13.7, 10.9 (CH_3) ppm. Anal. Calc. for $C_{19}H_{24}N_4O_3S$: C, 58.74; H, 6.23; N, 14.42. Found: C, 58.96; H, 6.01; N, 14.29%.

3.2. Synthesis of $CH_2{=}C(3,5\text{-}Me_2Pz)_2$

NaH (62 mg, 2.6 mmol) was added to the stirred solution of imidazole (0.18 g, 2.6 mmol) in THF (30 ml) at 0 °C. After stirring for 1 h at room temperature, $TsOCH_2CH(3,5\text{-}Me_2Pz)_2$ (1.01 g, 2.6 mmol) was added. The mixture was stirred and heated at reflux for 4 h. The solvent was evaporated and the residue was redissolved in CH_2Cl_2 (20 ml). The CH_2Cl_2 solution was washed with water (2×20 ml), and dried over anhydrous $MgSO_4$. The solvent was removed under reduced pressure and the residue was purified by column chromatography on silica with ethyl acetate as the eluent to give $CH_2{=}C(3,5\text{-}Me_2Pz)_2$ as a white solid. Yield: 0.25 g (45%). ^1H NMR: δ 5.90 (s, 2H, H^4 of pyrazole), 5.34 (s, 2H, CH_2), 2.25 (s, 6H, CH_3), 1.86 (s, 6H, CH_3) ppm. ^{13}C NMR: δ 150.6, 141.4 (C^3 and C^5 of pyrazole), 108.6 (C^4 of pyrazole), 139.9, 103.9 ($C{=}CH_2$), 14.3, 11.4 (CH_3) ppm. Anal. Calc. for $C_{12}H_{16}N_4$: C, 66.64; H, 7.46; N, 25.90. Found: C, 66.68; H, 7.78; N, 25.73%.

3.3. Synthesis of L^1–L^3

R_3SnH (2 mmol, R = *n*-Bu for **L**^{1}, $PhCH_2$ for **L**^{2} and Ph for **L**^{3}) was added the solution of $CH_2{=}C(3,5\text{-}Me_2Pz)_2$ (1 mmol) in anhydrous diethyl ether (30 ml). The reaction mixture was stirred for 36 h at room temperature, then the solvent was evaporated and the residue was redissolved in hexane (30 ml). The insoluble materials were filtered off, and hexane was removed under reduced pressure to give **L**^{1}–**L**^{3}.

Data for $(n\text{-}Bu)_3SnCH_2CH(3,5\text{-}Me_2Pz)_2$ (**L**^{1}). Colorless oil, yield: 96%. ^1H NMR: δ 6.47 (t, $J = 8.6$ Hz, 1H, C*H*), 5.75 (s, 2H, H^4 of pyrazole), 2.19 (s, 6H, CH_3), 2.04 (s, 6H, CH_3), 1.95 (d, $J = 8.6$ Hz, 2H, CH_2), 1.45–1.21 (m, 18H, protons of *n*-butyl), 0.86 (t, $J = 7.2$ Hz, 9H, CH_3) ppm. ^{13}C NMR: δ 146.4, 139.0 (C^3 and C^5 of pyrazole), 106.8 (C^4 of pyrazole), 74.1 (*C*H), 29.0, 27.4, 15.3, 13.6, 13.4, 10.8, 9.6 (carbons of CH_2, CH_3 and *n*-butyl) ppm. ^{119}Sn NMR: δ −22.2 ppm.

Data for $(PhCH_2)_3SnCH_2CH(3,5\text{-}Me_2Pz)_2$ (**L**^{2}). Colorless oil, yield: 95%. ^1H NMR: δ 7.16–7.07 (m, 9H, C_6H_5), 6.80–6.74 (m, 6H, C_6H_5), 6.12 (t, $J = 8.1$ Hz, 1H, C*H*), 5.80 (s, 2H, H^4 of pyrazole), 2.24 (s, 6H, CH_3), 2.20 (s, 6H, CH_2Ph), 1.84 (s, 6H, CH_3), 1.63 (d, $J = 8.1$ Hz, 2H, CH_2) ppm. ^{13}C NMR: δ 146.9, 142.4, 139.1, 128.4, 127.5, 123.4 (C^3 and C^5 of pyrazole as well as C_6H_5), 107.3 (C^4 of pyrazole), 72.4 (*C*H), 20.8, 17.5 (CH_2), 13.7, 10.7 (CH_3) ppm. ^{119}Sn NMR: δ −57.6 ppm.

Data for $Ph_3SnCH_2CH(3,5\text{-}Me_2Pz)_2$ (**L**^{3}). White solid, yield: 90%. ^1H NMR: δ 7.57–7.40 (m, 6H, C_6H_5), 7.31–7.28 (m, 9H, C_6H_5), 6.48 (t, $J = 8.3$ Hz, 1H, C*H*), 5.63 (s, 2H, H^4 of pyrazole), 2.55 (d, $J = 8.3$ Hz, 2H, CH_2), 2.04 (s, 6H, CH_3), 1.82 (s, 6H, CH_3) ppm. ^{13}C NMR: δ 147.1, 139.5, 139.4, 137.0, 128.7, 128.2 (C^3 and C^5 of pyrazole as well as C_6H_5), 107.2 (C^4 of pyrazole), 73.2 (*C*H), 18.0 (CH_2), 13.4, 10.7 (CH_3) ppm. ^{119}Sn NMR: δ −122.2 ppm. Anal. Calc. for $C_{30}H_{32}N_4Sn$: C, 63.51; H, 5.69; N, 9.88. Found: C, 63.53; H, 6.04; N, 10.30%.

3.4. Synthesis of L^4–L^7

R_3SnH (1 mmol, R = *n*-Bu for **L**^{4} and **L**^{6} as well as Ph for **L**^{5} and **L**^{7}) was added the solution of $CH_2{=}C(mim)_2$ (1 mmol, for **L**^{4} and **L**^{5}) or $CH_2{=}C(py)_2$ (1 mmol, for **L**^{6} and **L**^{7}) and AIBN (30 mg, 0.18 mmol) in THF (40 ml). After the reaction mixture was stirred and heated at reflux for 15 h, the solvent was removed under reduced pressure. The residue was purified by column chromatography on silica using ethyl acetate as the eluent to give **L**^{4}–**L**^{7}.

Data for $(n\text{-}Bu)_3SnCH_2CH(mim)_2$ (**L**^{4}). Colorless oil, yield: 57%. ^1H NMR: δ 6.91 (d, $J = 1.1$ Hz, 2H, protons of imidazole), 6.73 (d, $J = 1.1$ Hz, 2H, protons of imidazole), 4.64 (t, $J = 8.6$ Hz, 1H, C*H*), 3.46 (s, 6H, CH_3), 1.73 (d, $J = 8.6$ Hz, 2H, CH_2), 1.44–1.33 (m, 6H, protons of *n*-butyl), 1.31–1.19 (m, 6H, protons of *n*-butyl), 0.86 (t, $J = 7.2$ Hz, 9H, CH_3), 0.75–0.66 (m, 6H, protons of *n*-butyl) ppm. ^{13}C NMR: δ 147.3, 125.7, 120.7 (carbons of imidazole), 36.0 (*C*H), 31.9 (NCH_3), 28.1, 26.4, 12.7, 10.9, 8.1 (carbons of *n*-butyl and CH_2Sn) ppm. ^{119}Sn NMR: δ −14.7 ppm.

Data for $Ph_3SnCH_2CH(mim)_2$ (**L**^{5}). White solid, yield: 45%. ^1H NMR: δ 7.58–7.42 (m, 6H, C_6H_5), 7.32–7.28 (m, 9H, C_6H_5), 6.86 (d, $J = 0.9$ Hz, 2H, protons of imidazole), 6.58 (d, $J = 0.9$ Hz, 2H, protons of imidazole), 4.60 (t, $J = 8.6$ Hz, 1H, C*H*), 3.18 (s, 6H, CH_3), 2.34 (d, $J = 8.6$ Hz, 2H, CH_2) ppm. ^{13}C NMR: δ 147.8, 139.4, 137.1, 128.6, 128.1, 126.8, 122.0 (carbons of imidazole and C_6H_5), 36.7 (*C*H), 32.6 (NCH_3), 14.8 (CH_2) ppm. ^{119}Sn NMR: δ −108.4 ppm.

Data for $(n\text{-}Bu)_3SnCH_2CH(py)_2$ (**L**^{6}). Colorless oil, yield: 64%. ^1H NMR: δ 8.53 (d, $J = 4.8$ Hz, 2H, C_5H_4N), 7.58–7.53 (m, 2H, C_5H_4N), 7.32 (d, $J = 7.9$ Hz, 2H, C_5H_4N), 7.09–7.05 (m, 2H, C_5H_4N), 4.52 (t, $J = 8.3$ Hz, 1H, C*H*), 1.70 (d, $J = 8.3$ Hz, 2H, CH_2), 1.38–1.30 (m, 6H, protons of *n*-butyl), 1.26–1.16 (m, 6H, protons of *n*-butyl), 0.84 (t, $J = 7.2$ Hz, 9H, CH_3), 0.67–0.61 (m, 6H, protons of *n*-butyl) ppm. ^{13}C NMR: δ 165.0, 149.0, 136.3, 122.5, 121.3 (C_5H_4N), 53.7 (*C*H), 29.1, 27.4, 15.9, 13.7, 9.4 (carbons of *n*-butyl and CH_2Sn) ppm. ^{119}Sn NMR: δ −15.8 ppm.

Data for $Ph_3SnCH_2CH(py)_2$ (**L**^{7}). Colorless oil, yield: 53%. ^1H NMR: δ 8.32 (d, $J = 4.5$ Hz, 2H, C_5H_4N), 7.50–7.44 (m, 6H, C_6H_5), 7.42–7.39 (m, 2H, C_5H_4N), 7.29–7.23 (m, 9H, C_6H_5), 7.02–6.97 (m, 4H, C_5H_4N), 4.74 (t, $J = 7.7$ Hz, 1H, C*H*), 2.25 (d, $J = 7.7$ Hz, 2H, CH_2)

ppm. ^{13}C NMR: δ 163.8, 148.8 (C_5H_4N), 141.7, 137.0, 136.4, 128.1, 128.0, 122.9, 121.5 (carbons of C_5H_4N and C_6H_5), 52.1 (*C*H), 18.3 (CH_2) ppm. ^{119}Sn NMR: δ −120.9 ppm.

3.5. Reaction of L^1–L^3 with $W(CO)_5THF$

Ligands **L^1**–**L^3** (0.5 mmol) were added to the solution of $W(CO)_5THF$ in THF, prepared *in situ* by the irradiation of a solution of $W(CO)_6$ (0.5 mmol) in THF (40 ml) with a 300 W high-pressure Hg lamp for 8 h, and the reaction mixture was stirred and heated at reflux for 10 h. After the reaction was completed, the solvent was removed under a reduced pressure, and the residue was purified by column chromatography on silica using CH_2Cl_2/hexane (1:2, v/v) as the eluent to give complexes **1**–**3** as yellow solids.

Data for **1**. This complex was obtained by the reaction of **L^1** with $W(CO)_5THF$. Yield: 61%. ^{1}H NMR: δ 6.90 (t, *J* = 3.3 Hz, 1H, C*H*), 5.80 (s, 2H, H^4 of pyrazole), 2.46 (s, 6H, CH_3), 2.38 (s, 6H, CH_3), 1.57–1.47 (m, 6H), 1.37–1.25 (m, 8H), 1.20–1.14 (m, 6H) (CH_2 and protons of *n*-butyl), 0.86 (t, *J* = 7.3 Hz, 9H, CH_3) ppm. ^{13}C NMR: δ 191.1 (*C*O), 152.4, 137.1 (C^3 and C^5 of pyrazole), 106.9 (C^4 of pyrazole), 72.5 (*C*H), 36.3, 30.2, 27.5, 15.1, 15.0, 13.8, 11.5 (carbons of *C*H$_2$, *C*H$_3$ and *n*-butyl group) ppm. ^{119}Sn NMR: δ 86.5 ppm. IR: ν(CO) 1945 (vs), 1843 (vs), 1821 (vs) cm^{-1}. Anal. Calc. for $C_{27}H_{44}N_4O_3SnW$: C, 41.83; H, 5.72; N, 7.23. Found: C, 41.42; H, 5.45; N, 7.34%.

Data for **2**. This complex was obtained by the reaction of **L^2** with $W(CO)_5THF$. Yield: 45%. ^{1}H NMR: δ 7.01 (t, *J* = 7.4 Hz, 6H, C_6H_5), 6.88 (t, *J* = 7.1 Hz, 3H, C_6H_5), 6.73 (d, *J* = 7.4 Hz, 6H, C_6H_5), 6.57 (t, *J* = 3.1 Hz, 1H, C*H*), 5.81 (s, 2H, H^4 of pyrazole), 2.55 (s, 6H, CH_2Ph), 2.46 (s, 6H, CH_3), 2.30 (s, 6H, CH_3), 0.58 (d, *J* = 3.1 Hz, 2H, CH_2W) ppm. ^{13}C NMR: δ 223.4, 212.4 (*C*O), 152.4, 143.8, 137.4, 127.9, 127.8, 122.5 (C^3 and C^5 of pyrazole as well as C_6H_5), 107.0 (C^4 of pyrazole), 72.1 (*C*H), 33.2 (*C*H$_2$W), 24.0 (*C*H$_2$Sn), 15.1, 11.4 (*C*H$_3$) ppm. ^{119}Sn NMR: δ 69.4 ppm. IR: ν(CO) 1947 (vs), 1847 (vs), 1827 (vs) cm^{-1}. Anal. Calc. for $C_{36}H_{38}N_4O_3SnW$: C, 49.29; H, 4.37; N, 6.39. Found: C, 49.46; H, 4.08; N, 6.54%.

Data for **3**. This complex was obtained by the reaction of **L^3** with $W(CO)_5THF$. Yield: 41%. ^{1}H NMR: δ 7.65–7.49 (m, 6H, C_6H_5), 7.33–7.28 (m, 9H, C_6H_5), 6.81 (t, *J* = 3.3 Hz, 1H, C*H*), 5.86 (s, 2H, H^4 of pyrazole), 2.55 (s, 6H, CH_3), 2.36 (s, 6H, CH_3), 1.32 (d, *J* = 3.3 Hz, 2H, CH_2) ppm. ^{13}C NMR: δ 152.9, 144.9, 137.6, 137.4, 136.1, 127.8 (C^3 and C^5 of pyrazole as well as C_6H_5), 107.3 (C^4 of pyrazole), 72.4 (*C*H), 38.3 (*C*H$_2$), 15.1, 11.5 (*C*H$_3$) ppm. The signals of carbonyl carbons were not observed attributed to their low intensity and relatively low solubility of this complex. ^{119}Sn NMR: δ 22.1 ppm. IR: ν(CO) 1958 (vs), 1865 (vs), 1831 (vs) cm^{-1}. Anal. Calc. for $C_{33}H_{32}N_4O_3SnW$: C, 47.46; H, 3.86; N, 6.71. Found: C, 47.21; H, 3.73; N, 6.62%.

3.6. Reaction of L^4 and L^5 with $W(CO)_6$

L^4 or **L^5** (0.5 mmol) was added to a solution of $W(CO)_6$ in dioxane (30 ml). After the reaction mixture was stirred and heated at reflux for 15 h, the solvent was removed under a reduced pressure, and the residue was purified by column chromatography on silica using CH_2Cl_2/hexane (2:1, v/v) as the eluent to give complex **4** or **5** as a yellow solid.

Data for **4**. This complex was obtained by the reaction of **L^4** with $W(CO)_6$. Yield: 57%. ^{1}H NMR: δ 7.31 (s, 2H, protons of imidazole), 6.79 (s, 2H, protons of imidazole), 4.39 (t, *J* = 8.6 Hz, 1H, C*H*), 3.72 (s, 6H, CH_3), 1.57 (d, *J* = 8.6 Hz, 2H, CH_2), 1.41–1.39 (m, 6H, protons of *n*-butyl), 1.33–1.22 (m, 6H, protons of *n*-butyl), 0.88 (t, *J* = 7.2 Hz, 9H, CH_3), 0.73–0.69 (m, 6H, protons of *n*-butyl) ppm. ^{13}C NMR: δ 213.8, 202.4 (*C*O), 147.1, 133.3, 120.9 (carbons of imidazole), 33.7, 31.3, 29.0, 27.3, 13.6, 12.3, 9.2 (carbons of *n*-butyl, *C*H, *C*H$_2$ and *C*H$_3$) ppm. ^{119}Sn NMR: δ −15.8 ppm. IR: ν(CO) 1997 (s), 1882 (vs), 1851 (vs), 1801 (vs) cm^{-1}. Anal. Calc. for $C_{26}H_{40}N_4O_4SnW$: C, 40.29; H, 5.20; N, 7.23. Found: C, 39.91; H, 5.33; N, 7.70%.

Data for **5**. This complex was obtained by the reaction of **L^5** with $W(CO)_6$. Yield: 54%. ^{1}H NMR: δ 7.51–7.33 (m, 15H, C_6H_5), 7.23 (s, 2H, protons of imidazole), 6.47 (s, 2H, protons of imidazole), 4.48 (t, *J* = 8.3 Hz, 1H, C*H*), 3.36 (s, 6H, CH_3), 2.33 (d, *J* = 8.3 Hz, 2H, CH_2) ppm. ^{13}C NMR (DMSO-d_6): δ 213.4, 206.7, 202.5 (*C*O), 147.1, 137.2, 136.2, 130.9, 129.0, 128.6, 122.2 (carbons of imidazole and C_6H_5), 33.3 (*C*H$_3$), 30.0 (*C*H), 13.5 (*C*H$_2$) ppm. ^{119}Sn NMR: δ −116.1 ppm. IR: ν(CO) 1997 (s), 1867 (vs), 1844 (vs), 1805 (vs) cm^{-1}. Anal. Calc. for $C_{32}H_{28}N_4O_4SnW$: C, 46.02; H, 3.38; N, 6.71. Found: C, 45.77; H, 3.31; N, 7.07%.

3.7. Reaction of L^6 and L^7 with $W(CO)_5THF$

These reactions were similarly carried out as above-mentioned reactions of **L^1**–**L^3** with $W(CO)_5THF$. After purification through column chromatography on silica using CH_2Cl_2/hexane (1:1, v/v) as the eluent, complex **6** from **L^6** and complex **7** from **L^7** were obtained as yellow-green solids.

Data for **6**. Yield: 43%. ^{1}H NMR: δ 9.16 (d, *J* = 5.2 Hz, 2H, C_5H_4N), 7.80 (t, *J* = 7.3 Hz, 2H, C_5H_4N), 7.60 (d, *J* = 8.0 Hz, 2H, C_5H_4N), 7.11 (t, *J* = 6.4 Hz, 2H, C_5H_4N), 4.70 (t, *J* = 8.3 Hz, 1H, C*H*), 1.71 (d, *J* = 8.3 Hz, 2H, CH_2), 1.38–1.21 (m, 12H, protons of *n*-butyl), 0.86 (t, *J* = 7.1 Hz, 9H, CH_3), 0.78–0.68 (m, 6H, protons of *n*-butyl) ppm. ^{13}C NMR: δ 214.3, 206.2, 201.8 (CO), 162.8, 155.6, 138.1, 122.3, 122.1 (C_5H_4N), 55.0 (*C*H), 29.0, 27.3, 13.6, 10.2, 9.7 (carbons of *n*-butyl and *C*H$_2$Sn) ppm. ^{119}Sn NMR: δ −12.4 ppm. IR: ν(CO) 2000 (s), 1895 (vs), 1866 (vs), 1816 (vs) cm^{-1}. Anal. Calc. for $C_{28}H_{38}N_2O_4SnW$: C, 43.72; H, 4.98; N, 3.64. Found: C, 44.11; H, 5.17; N, 3.52%.

Data for **7**. Yield: 45%. ^{1}H NMR: δ 9.20 (d, *J* = 5.2 Hz, 2H, C_5H_4N), 7.76 (dt, *J* = 1.1 Hz, *J* = 7.6 Hz, 2H, C_5H_4N), 7.54–7.46 (m, 8H, C_5H_4N and C_6H_5), 7.23–7.20 (m, 9H, C_6H_5), 7.19–7.16 (m, 2H, C_5H_4N), 5.28 (t, *J* = 3.2 Hz, 1H, C*H*), 1.70 (d, *J* = 3.2 Hz, 2H, CH_2) ppm. ^{13}C NMR: δ 196.2 (CO), 167.2, 154.4, 139.5, 137.3, 136.1, 129.2, 127.7, 123.0, 121.6 (C_5H_4N and C_6H_5), 57.6 (*C*H), 29.7 (*C*H$_2$) ppm. ^{119}Sn NMR: δ 22.8 ppm. IR: ν(CO) 1961 (s), 1857 (s), 1829 (vs) cm^{-1}. Anal. Calc. for $C_{33}H_{26}N_2O_3SnW$: C, 49.47; H, 3.27; N, 3.50. Found: C, 49.23; H, 3.62; N, 3.57%.

3.8. Reaction of L^7 with $W(CO)_6$

The solution of **L^7** (0.5 mmol) with $W(CO)_6$ (0.5 mmol) in THF (40 ml) was irradiated with a 300 W high-pressure Hg lamp for 8 h. The solvent was removed under a reduced pressure, and the residue was isolated by column chromatography on silica using CH_2Cl_2/hexane (1:2, v/v) as the eluent firstly to give **7** in 11% yield, then CH_2Cl_2/hexane (1:1, v/v) as the eluent to give **8** in 28% yield. Data for **8**. ^{1}H NMR: δ 9.01 (d, *J* = 5.4 Hz, 2H, C_5H_4N), 7.69–7.52 (m, 6H, C_6H_5), 7.45–7.31 (m, 13H, C_5H_4N and C_6H_5), 7.03–6.98 (m, 2H, C_5H_4N), 4.75 (t, *J* = 8.4 Hz, 1H, C*H*), 2.36 (d, *J* = 8.4 Hz, 2H, CH_2) ppm. ^{13}C NMR: δ 214.4, 205.9, 202.0 (*C*O), 161.7, 155.5, 138.1, 136.9, 136.7, 129.4, 128.9, 122.3, 122.2 (C_5H_4N and C_6H_5), 54.4 (*C*H), 12.9 (*C*H$_2$) ppm. ^{119}Sn NMR: δ −110.7 ppm. IR: ν(CO) 2004 (s), 1881 (sh), 1865 (vs), 1810 (vs) cm^{-1}. Anal. Calc. for $C_{34}H_{26}N_2O_4SnW$: C, 49.25; H, 3.16; N, 3.38. Found: C, 48.98; H, 3.38; N, 3.44%.

3.9. Reaction of 6 and 7 with I_2

I_2 (0.062 mmol) was added to the stirred solution of **6** or **7** (0.062 mmol) in CH_2Cl_2 (15 ml). The reaction mixture was stirred at room temperature for 4 h. The solvent was removed under a reduced pressure, and the residue was purified by column chromatography on silica using CH_2Cl_2/hexane (2:1, v/v) as the eluent to give **9** as a yellow solid. Yield: 35% from **6** to 45% from **7**, respectively. ^{1}H NMR (acetone-d_6): δ 9.56 (d, *J* = 5.6 Hz, 2H, C_5H_4N), 8.09

Table 1
Crystal data and refinement parameters for complexes **2**–**4**, **6**, **7** and **9**.

Complex	2	3.1.5CH_2Cl_2	4	6	7	9
Formula	$C_{36}H_{38}N_4O_3SnW$	$C_{34.5}H_{35}Cl_3N_4O_3SnW$	$C_{26}H_{40}N_4O_4SnW$	$C_{28}H_{38}N_2O_4SnW$	$C_{33}H_{26}N_2O_3SnW$	$C_{15}H_{11}IN_2O_3W$
Formula weight	877.24	962.56	775.16	769.14	801.10	578.01
Crystal size (mm)	0.22 × 0.20 × 0.18	0.20 × 0.20 × 0.10	0.20 × 0.18 × 0.12	0.14 × 0.12 × 0.10	0.20 × 0.18 × 0.10	0.21 × 0.19 × 0.18
Crystal system	Monoclinic	Monoclinic	Triclinic	Triclinic	Orthorhombic	Triclinic
Space group	$P2_1/n$	$P2_1/n$	$P\bar{1}$	$P\bar{1}$	*Pnma*	$P\bar{1}$
a (Å)	11.334 (2)	11.174 (4)	8.1837 (16)	8.3053 (4)	11.241 (2)	7.410 (2)
b (Å)	13.634 (3)	15.315 (5)	9.5802 (19)	9.3753 (4)	14.486 (3)	8.903 (2)
c (Å)	25.964 (5)	20.917 (6)	21.539 (4)	20.9579 (12)	17.857 (4)	13.463 (3)
α (°)	90	90	79.64 (3)	91.062 (5)	90	106.94 (3)
β (°)	102.24 (3)	91.905 (4)	81.66 (3)	91.468 (4)	90	92.62 (3)
γ (°)	90	90	67.88 (3)	115.886 (5)	90	108.44 (3)
T (K)	113 (2)	113 (2)	293 (1)	122 (1)	294 (2)	293 (2)
V (Å)^3	3921.1 (14)	3578 (2)	1533.3 (6)	1466.9 (1)	2907.8 (10)	796.6 (3)
Z	4	4	2	2	4	2
D_c (g.cm^{-3})	1.486	1.787	1.679	1.741	1.830	2.410
F (000)	1720	1876	760	752	1544	532
μ (mm^{-1})	3.603	4.174	4.597	4.803	4.848	9.201
θ Range (°)	2.19–27.92	1.65–27.92	1.93–27.997	2.90–25.01	3.24–26.00	3.12–25.00
No. of measured reflections	36118	32282	13759	5152	18223	6979
No. of unique reflections (R_{int})	9214 (0.0780)	8516 (0.0427)	7162 (0.0448)	5152 (0.0503)	2965 (0.0605)	2809 (0.0582)
No. of observed reflections with ($I > 2\sigma(I)$)	7307	7027	5070	4628	2663	2527
No. of parameters	411	437	434	328	199	200
GOF	1.034	1.024	1.026	1.060	1.324	1.041
Residuals R_1, wR_2	0.0517, 0.1229	0.0231, 0.0464	0.0555, 0.1351	0.0558, 0.1480	0.0534, 0.1350	0.0344, 0.0665

(dt, $J = 1.6$ Hz, $J = 7.7$ Hz, 2H, C_5H_4N), 7.96 (d, $J = 7.8$ Hz, 2H, C_5H_4N), 7.50 (ddd, $J = 1.3$ Hz, $J = 5.6$ Hz, $J = 7.2$ Hz, 2H, C_5H_4N), 5.59 (t, $J = 3.1$ Hz, 1H, *CH*), 2.32 (d, $J = 3.1$ Hz, 2H, CH_2) ppm. ^{13}C NMR (acetone-d_6): δ 226.8 (*CO*), 163.9, 156.3, 141.2, 124.1, 122.0 (C_5H_4N), 60.9 (*CH*), 45.0 (CH_2) ppm. IR: ν(CO) 1996 (vs), 1879 (vs) cm^{-1}. Anal. Calc. for $C_{15}H_{11}IN_2O_3W$: C, 31.17; H, 1.92; N, 4.85. Found: C, 31.47; H, 2.23; N, 4.75%.

3.10. Crystal structure determinations

Yellow crystals of **2**–**4**, **6**, **7** and **9** suitable for X-ray analyses were obtained by slow diffusion of hexane into their CH_2Cl_2 solutions at −18 °C. All intensity data were collected on a SuperNova Eos detector for **6** and **9** as well as Rigaku Saturn CCD detector for **2**–**4** and **7** using Mo-Kα radiation ($\lambda = 0.71073$ Å). All calculations were carried out using Olex2 [32]. Semi-empirical absorption corrections were applied using the Crystalclear program [33]. The structures were solved by direct methods and difference Fourier map using SHELXS of the SHELXTL package and refined with SHELXL [34] by full-matrix least-squares on F^2. All non-hydrogen atoms were refined anisotropically. Hydrogen atoms were added geometrically and refined with riding model position parameters. The butyl groups were disordered in **4**. The occupancy factors were refined to 0.5 for C(15)–C(26). A summary of the fundamental crystal data for these complexes is listed in Table 1.

Acknowledgments

This work is supported by the National Natural Science Foundation of China (No. 21372124).

Appendix A. Supplementary data

Supplementary data to this article can be found online at https://doi.org/10.1016/j.jorganchem.2018.11.029.

References

[1] M.M. Heravi, L. Mohammadkhani, Recent applications of Stille reaction in total synthesis of natural products: an update, J. Organomet. Chem. 869 (2018) 106–200.
[2] C. Cordovilla, C. Bartolomé, J.M. Martínez-Ilarduya, P. Espinet, The Stille reaction, 38 years later, ACS Catal. 5 (2015) 3040–3053.
[3] J.K. Stille, The palladium-catalyzed cross-coupling reactions of organotin reagents with organic electrophiles, Angew. Chem., Int. Ed. Engl. 25 (1986) 508–524.
[4] S.D. Wobser, C.J. Stephenson, M. Delferro, T.J. Marks, Carbostannolysis mediated by bis(pentamethylcyclopentadienyl)lanthanide catalysts. Utility in accessing organotin synthons, Organometallics 32 (2013) 1317–1327.
[5] H. Yoshida, Stannylation reactions under base metal catalysis: some recent advances, Synthesis 48 (2016) 2540–2552.
[6] T. Matsubara, Density functional study on the carbostannylation of aryne by the palladium(0)-iminophosphine catalyst. Does the apical site really contribute to the catalytic reaction? Organometallics 22 (2003) 4297–4304.
[7] T. Matsubara, Density functional study on the mechanism of the oxidative addition of the highly polarized Sn–C σ-bond to the (LH_3)(L'H_3)Pd and ($LH_2C_2H_4LH_2$)Pd (L,L' = N, P, As, Sb) complexes, Organometallics 22 (2003) 4286–4296.
[8] E. Wächtler, S. Wahlicht, S.H. Privér, M.A. Bennett, B. Gerke, R. Pöttgen, E. Brendler, R. Gericke, J. Wagler, S.K. Bhargava, Tin(IV) compounds with 2-$C_6F_4PPh_2$ substituents and their reactivity toward palladium(0): formation of tin–palladium complexes via oxidative addition, Inorg. Chem. 56 (2017) 5316–5327.
[9] H. Kameo, S. Ishii, H. Nakazawa, Facile synthesis of rhodium and iridium complexes bearing a [PEP]-type ligand (E = Ge or Sn) via E–C bond cleavage, Dalton Trans. 41 (2012) 11386–11392.
[10] Y.-F. Xie, G.-T. Zeng, H.-B. Song, L.-F. Tang, The modification of $ArSCH_2$(3,5-Me_2Pz) (Ar = phenyl or 2-pyridyl, Pz = pyrazol-1-yl) by organotin group and related reactions, J. Organomet. Chem. 695 (2010) 2172–2179.
[11] L.-F. Tang, W.-L. Jia, D.-T. Song, Z.-H. Wang, J.-F. Chai, J.-T. Wang, An unprecedented κ^3-[N,C,N] coordination mode of the bis(3,4,5-trimethylpyrazol-1-yl) methide ligand, Organometallics 21 (2002) 445–447.
[12] D. Kruber, K. Merzweiler, C. Wagner, H. Weichmann, Ligand behaviour of P-functionally substituted organotin halides: synthesis, structure, and intramolecular oxidative addition of [{Me_2(Cl)$SnCH_2CH_2PPh_2$}$_2$Rh(CO)Cl], J. Organomet. Chem. 572 (1999) 117–123.
[13] B.P. Buffin, M.J. Poss, A.M. Arif, T.G. Richmond, Synthesis and reactivity of a W(0) anion stabilized by chelating tertiary amines. Oxidative addition and reductive elimination of a carbon-tin bond at tungsten, Inorg. Chem. 32 (1993) 3805–3806.
[14] C. Müller, U. Schubert, Transition metal stannyl complexes, 4. -Palladium and platinum complexes with chelating phosphinoalkylstannyl ligands by oxidative addition of Sn–C bonds, Chem. Ber. 124 (1991) 2181–2184.
[15] D. Das, S.S. Mohapatra, S. Roy, Recent advances in heterobimetallic catalysis across a "transition metal–tin" motif, Chem. Soc. Rev. 44 (2015) 3666–3690.
[16] M.S. Holt, W.L. Wilson, J.H. Nelson, Transition metal–tin chemistry, Chem. Rev. 89 (1989) 11–49.
[17] L.-F. Tang, S.-B. Zhao, W.-L. Jia, Z. Yang, D.-T. Song, J.-T. Wang, Reaction of bis(pyrazol-1-yl)methanes modified by organotin groups on the methine carbon with $W(CO)_5$THF to give novel heterodinuclear organometallic complexes, Organometallics 22 (2003) 3290–3298.

[18] Y.-F. Xie, Z.-K. Wen, R.-Y. Tan, J. Hong, S.-B. Zhao, L.-F. Tang, bis(3,5-dimethylpyrazol-1-yl)acyl and bis(3,5-dimethylpyrazol-1-yl)methide carbonyl tungsten derivatives, Organometallics 27 (2008) 5684–5690.
[19] S.S. Batsanov, Van der Waals radii of elements, Inorg. Mater. 37 (2001) 1031–1046.
[20] X.-Y. Zhang, K. Ding, H.-B. Song, L.-F. Tang, Reactivity of $(mim)_2C{=}O$, $(mim)_2CH_2$ and $(mim)_2C{=}CH_2$ (mim = 1-methylimidazole-2-yl) with group 6 metal carbonyl complexes, Chin. J. Inorg. Chem. 26 (2010) 1–7.
[21] L.E. Orgel, The infrared spectra of substituted metal carbonyls, Inorg. Chem. 1 (1962) 25–29.
[22] Q. Ye, Q. Wu, H. Zhao, Y.-M. Song, X. Xue, R.-G. Xiong, S.-M. Pang, G.-H. Lee, Two noncentrosymmetric complexes: $[W(CO)_4(bipy)]$ and $[W(CO)_4(phen)]$(bipy = 2,2'-bipyridine, phen = 1,10-phenanthroline) obtained through solvothermal synthesis and their optical properties, J. Organomet. Chem. 690 (2005) 286–290.
[23] S.H.L. Thoonen, B.-J. Deelman, G. van Koten, Synthetic aspects of tetraorganotins and organotin(IV) halides, J. Organomet. Chem. 689 (2004) 2145–2157.
[24] S. Dilsky, Molybdenum and tungsten complexes of the neutral tripod ligands $HC(pz)_3$ and $MeC(CH_2PPh_2)_3$, J. Organomet. Chem. 692 (2007) 2887–2896.
[25] I.K. Dhawan, M.A. Bruck, B. Schilling, C. Grittini, J.H. Enemark, Mononuclear and binuclear molybdenum complexes of the tris(3,5-dimethyl-l-pyrazolyl) methane ligand, Inorg. Chem. 34 (1995) 3801–3808.
[26] K.-B. Shiu, K.-S. Liou, S.-L. Wang, S.-C. Wei, Organotransition-metal complexes of multidentate ligands. 10.[1] Steric vs electronic control on formation of six- and seven-coordinate carbonyl halides of molybdenum(II) and tungsten(II), Organometallics 9 (1990) 669–675.
[27] S.D. Perera, J.J. Fernandez-Sanchez, B.L. Shaw, Activation of C–X (X=Cl or Br) bonds in 2-halobenzaldehydes, as their 2-pyridylhydrazone derivatives: oxidative addition to tungsten(0) to give aryl–tungsten(II) complexes, Inorg. Chim. Acta. 325 (2001) 175–178.
[28] S.D. Perera, B.L. Shaw, Cyclometallation of 2-halogenobenzaldehyde mixed azine phosphines of type $PPh_2CH_2C(^tBu){=}N\text{-}N{=}CH(C_6H_4X\text{-}2)$ (X = I, Br or Cl) involving facile C-X bond fission at tungsten(0), J. Organomet. Chem. 479 (1994) 117–124.
[29] T.G. Richmond, M.A. Klng, E.P. Kelson, A.M. Arlt, Facile chelate assisted carbon-halogen bond cleavage at tungsten(0), Organometallics 6 (1987) 1995–1996.
[30] A. Otero, J. Fernández-Baeza, J. Tejeda, A. Antiñolo, F. Carrillo-Hermosilla, E. Díez-Barra, A. Lara-Sánchez, M. Fernández-López, A new type of mono-anionic “scorpionate” ligand. Synthesis, spectroscopic characterisation and dynamic behaviour of some niobium(III) complexes, J. Chem. Soc., Dalton Trans. (2000) 2367–2374.
[31] G.J. Summers, M.P. Ndawuni, C.A. Summers, Dipyridyl functionalized polysulfones for membrane production, J. Membr. Sci. 226 (2003) 21–33.
[32] O.V. Dolomanov, L.J. Bourhis, R.J. Gildea, J.A.K. Howard, H. Puschmann, OLEX2: a complete structure solution, refinement and analysis program, J. Appl. Crystallogr. 42 (2009) 339–341.
[33] CrystalStructure 3.7.0 and Crystalclear 1.36: Crystal Structure Analysis Package, Rigaku and Rigaku/MSC, TX, 2000–2005.
[34] G.M. Sheldrick, A short history of SHELX, Acta Crystallogr. A64 (2008) 112–122.